Hydraulic fracturing experiments in vertical boreholes in the German Creek coal seam

by

R.G. Jeffrey[1], J.R. Enever[1], R. Phillips[2], D. Moelle[2], and S. Davidson[3]

[1]CSIRO Division of Geomechanics, [2]Capricorn Coal Management Pty Ltd, [3]North Queensland Energy Pty Ltd.

INTRODUCTION

Hydraulic fracturing is the most commonly used method to stimulate production from coalbed methane wells. In the U.S., thousands of fracture stimulations have been performed. Despite this substantial experience base, problems are still often encountered in performing fracture treatments to design specifications. Fracture design models are not able to predict treating pressure, fracture geometry, and propped length with any reliability. Design practice is to incrementally adapt designs that have been pumped successfully to improve their performance. This practice is a valid and useful exercise, but its use indicates that hydraulic fracturing processes in coal are not well understood.

This paper summarizes results from a set of three field experiments that were conducted to investigate hydraulic fracturing of coal. Each fracturing experiment included a site characterization phase during which stress, rock, reservoir and other properties were measured. This data was later compared and correlated with the recorded treating parameters and with the fracture geometry mapped during and after mining.

Stimulation by Fracturing

The goal of any stimulation method is to increase the rate that reservoir fluids can be produced from a well. Hydraulic fracturing does this by creating a propped fracture in the reservoir that is highly permeable compared to the reservoir rock. In an unfractured well, the reservoir fluids are produced through the rock surface area at the wellbore, exposed by drilling of the borehole through the reservoir formation. In a hydraulically fractured well, reservoir fluids are produced through the surface area of the hydraulic fracture, which is usually thousands of times the surface area of the wellbore.

An effective fracture must be both highly permeable and of sufficient width, compared with the permeability and exposed area of the reservoir rock, to allow the fluids produced to easily flow within the fracture to the wellbore. The fracture then effectively acts as a low-pressure conduit or drain that extends from the wellbore into the reservoir rock.

A poorer than planned stimulation can result from a number of things:

1. The reservoir may be damaged by the fluid injected into it during the fracturing operations. For example, it has been suggested that organic-based gels when used as fracturing fluids in coal stimulations can damage the permeability of the coal by chemically bonding to the coal and causing it to swell (Puri *et al.*, 1991).

2. The fracture may not have a geometry that contacts enough coal seam surface area through which to produce the water and gas. The hydraulic fracture should propagate in the seam, or in a permeable adjacent rock layer, so that water and gas can be produced from a large area of reservoir material into the low-pressure channel provided by the propped fracture.

3. The fracture conductivity (product of fracture width and proppant permeability) may be so low that reservoir fluids cannot flow freely back to the well. Proppant permeability is damaged by fracturing fluid residues and by plugging of flow paths by fine coal or clay particles that are present in the seam or are formed by the fracturing processes.

Location

The fracturing experiments described in this paper were conducted at the German Creek Mine Central Colliery which is located in Central Queensland, about 200 km west of Rockhampton. A plan of Central Colliery is shown in Figure 1. The locations of the boreholes in which the fracturing experiments were carried out are shown as is the hole, ECC 90, in which a full-scale treatment was performed in March, 1989 (Jeffrey *et al.*, 1992).

SITE CHARACTERIZATION

Each borehole was drilled using a 102-mm rotary bit until the hole was about 10 metres from the top of the German Creek coal seam. HQ sized core, which leaves a 96 mm diameter hole, was then taken through the seam to 6 to 8 metres below the bottom of the seam. Geophysical logs were run over the lower part of the hole and the in-seam location of borehole was determined by running a verticality log. The core was geologically logged and then used to select sites for stress testing. Core based hydraulic fracture strength and elastic property tests were later conducted in the lab. Mechanical properties determined from testing the core are given in Table 1.

Well Testing

A well test is run in the coal seam to measure the seam permeability and initial reservoir pressure. The test consists of injecting clean water for 2.5 to 3 hours while monitoring and recording the resulting pressure build up in the borehole. The test section is then shut in and the pressure fall off is recorded. Table 2 summarizes the well test results for all boreholes tested during this project.

Stress Testing

The in-situ stress field strongly affects the geometry and orientation of hydraulic fractures (Geertsma, 1989; Nolte and Smith, 1981). Microhydraulic fracture stress tests (Enever and Wooltorton, 1986) were used in each hole to measure the stresses in the rock above and below the seam. Prior to each main fracturing experiment in the seam, step-rate tests were run to determine the magnitude of the minimum principal stress in the seam. Table 3 summarizes the stress test results for the three boreholes that were fractured.

The horizontal stress field in the roof rocks was imbalanced and the minimum principal horizontal stress was higher in magnitude in the floor rock than in the roof rock at all sites. The reason for this is unclear at this time, but it reflects a significant change in the in-situ stress field across the coal seam. The mid-seam and other shear zones that are found in the German Creek seam at Central Colliery are evidence of differential movement across the coal seam resulting in differences in the stress fields above and below the seam.

Fluid Loss Testing

A minifrac test was run before each main experiment. This test consisted of injecting 3,000 to 4,000 litres of the selected crosslinked HPG fracturing fluid at injection rates similar to the planned rate for the main experiment. The injection part of the test is used to give information about treating pressures and fracture geometry growth behavior and the shut-in period of the test is analyzed to provide an estimate of the leakoff coefficient (Nolte, 1989). The falloff data from this test is also useful for determining fracture closure values. Table 4 gives leakoff coefficient values determined for ECC 87 and DDH 189 and 190 from the minifrac tests run.

The leakoff coefficients were calculated assuming a simple fracture geometry and a pressure-independent leakoff process. Though these assumptions do not hold for hydraulic fractures in coal (Warpinski, 1991), the leakoff coefficients were calculated to provide another basis for comparison between the three sites.

Discussion

The site characterization work, summarized above, revealed that site conditions were considerably different between ECC 87 and the other two boreholes. ECC 87 was located in about the center of the 305 longwall panel and, at the time of the testing the longwall face was only a little over 100 metres south of the in-seam location of the borehole. Development roadways were located about 100

metres to the east and west of ECC 87 and, because of the nearness of these mine openings, the reservoir pressure in the seam was very low (about 0.2 MPa). In contrast, DDH 189 and 190 were both more than 400 metres from the nearest mine opening when they were tested and the measured reservoir pressures in the seam at these locations were higher (though still lower than expected based on measurements made over a number of years in other boreholes).

The stress field in the floor rocks was similar at the three sites while the stress field in the roof rocks varied significantly, with s_{Hmin} decreasing progressively from ECC 87 to DDH 189 and DDH 190. In the roof rock at ECC 87, σ_{Hmin} was greater than the vertical stress in magnitude while at both DDH 189 and 190 σ_{Hmin} in the roof rock was considerably less than the vertical stress magnitude. Such low horizontal stresses have not previously been measured at German Creek (Enever and Wooltorton, 1986). A syncline axis runs through the region of DDH 189 and 190 and the observed trend at these sites of σ_{Hmin} increasing in magnitude upward from the seam is consistent with flexure of the rock layers by the syncline generating forces. In contrast, the horizontal stress field in the floor rock remained greater than the vertical stress in magnitude at all three sites. Such a change in stress across a low-shear strength layer is consistent with stress changes resulting from bending of laminated composite plates and beams (Heller and Swift, 1971). Bending of such a composite plate model provides a reasonable explanation for the observed stresses, but additional stress measurements and modeling are required before it can be accepted as the explanation.

Fracture growth into the roof is favoured by a state of in-situ stress such as exists at the DDH 189 and 190 sites; the magnitude of the minimum principal horizontal stress was higher in the coal than in roof rock. Growth of a hydraulic fracture vertically out of the coal seam is strongly influenced by the stress contrasts existing between the stress in the coal seam and the over- and underlying rock layers. Simonson, *et al.*, (1978) presented an analysis for a three layer system which employed a superposition of the internal pressure acting to open and extend the fracture and the external stresses acting to close the fracture. For the fracture to extend, the resulting excess pressure acting in the fracture must result in a stress intensity factor equal to the fracture toughness of the rock. A vertical cross section through a fracture growing in height into layers that contain higher stresses is shown in Figure 2. For this case, the relationship between the stress contrast between the low and higher stressed layers and fracture height is given by (Geertsma, 1989).

$$\sigma_{hb} - \sigma_{hc} = \frac{\pi}{2} \frac{\left[\frac{K_{Ic}\sqrt{2}}{\sqrt{h_f \pi}} + \sigma_{hb} - P \right]}{\sin^{-1}\left(\frac{h_r}{h_f} \right)} \quad (1)$$

In this equation, K_{Ic} is the fracture toughness of the rock, σ_{hb} and σ_{hc} are the minimum principal stresses in the rock and coal respectively, h_r is the height of the reservoir (coal seam thickness), h_f is the height of the fracture, and P is the pressure in the fracture, assumed to act uniformly over the entire vertical section. Figure 3 shows a plot of fracture height versus pressure in the fracture for the case of a 2.5 metre-thick coal seam and assuming a fracture toughness of 1.0 MPa $\sqrt{(m)}$. The pressure shown is the pressure in the fracture in excess of σ_{hc}. This type of relationship is incorporated, with model-dependent modifications, into many pseudo-3D hydraulic fracturing design models as a part of the height growth calculation. As can be seen from equation 1, this calculation simplifies the problem, ignoring material property contrasts, interface blunting and shear effects, and fluid loss contrasts. In addition, if the horizontal stresses in the layers above and below the coal are higher in magnitude than the vertical stress, a hydraulic fracture that grows into these layers will eventually reorient itself and become horizontal.

FRACTURING EXPERIMENTS

The fracturing experiments are small-scale compared with full-scale commercial fracturing treatments. Table 5 lists volumes and rates typical of these small-scale and commercial full-scale treatments.

The boreholes were drilled near and ahead of mine workings at the Central Colliery of

the German Creek Mine. Minethrough of the fractures occurred within less than one year after completing the surface work for all three experiments. During and after mining passed through the fracture, the fracture geometry was mapped and samples of coal and proppant were taken.

These fracture treatments used a borate crosslinked hydroxypropyl guar (HPG) fracturing fluid which is non-Newtonian and shear-thinning. The fluid was mixed by adding 4.8 kg of HPG per 1,000 litres of water (40 lbs per 1,000 U.S. gallons). The crosslinker activator, which is a sodium hydroxide solution, is added to the high pressure line near the well head. The published power-law rheology parameters for the fluid as mixed are n' = 0.48, K' = 0.185 $lb_f sec^{n'}/ft^2$ at 37.8°C which gives an apparent viscosity of 610 centipoise at a shear rate of 170 $sec.^{-1}$ This fluid is the same as used in many commercial fracturing treatments.

For the slurry stages, glass beads and sand are added at a paddle blender and the slurry is fed from the blender to the suction side of the high pressure triplex pump by centrifugal slurry pumps. The triplex then pumps the fluid through the surface hoses and flow meter/densitometer module to the well head and from there down the tubular string in the borehole to the coal seam. A string of BQ drill rods is used in the borehole to carry the fluid to the depth of the seam where an inflatable packer isolates the coal seam. A downhole pressure transducer is located in a housing just above the packer and measures the pressure in the rod string at that point. Figure 4 is a drawing of the surface and downhole equipment used during the hydraulic fracturing experiment.

Treatment Data

Summary plots of pressure, injection rate, and proppant concentration in the fluid are shown in Figures 5, 6, and 7. A valve problem with the activator pump meant that no crosslinking occurred in the treatment in ECC 87 until about one quarter of the fluid had been injected. The rapid increase in pressure seen in Figure 5 at this point is associated with increased flow resistance, mostly in the fracture, to the crosslinked fluid compared with the non-crosslinked linear gel. The experiments are summarized in Table 6.

All three treatments displayed the trend of increasing bottom-hole pressure with time. Nolte-Smith plots of the treatments were made and the slope of the log of net pressure versus log of elapsed time near the end of each experimental treatment are given in Table 7 below along with the bottom-hole pressure drop recorded at shut-in.

Discussion of Treatments

Borehole ECC 87, after crosslinking began, treated with a high and increasing bottom-hole pressure. At shut-in a pressure drop of about 1 MPa occurred. Thus, the observed pressure is believed to be mostly caused by fluid friction distributed over most of the extent of the fracture geometry and by a gel-out condition at the fracture tip. Closure was forced by flowing the well back. Upon shutting the flow-back valve, the pressure rebounded to a value equal to the overburden stress though the value of $s_{H\,min}$ in the roof rock was close in magnitude to overburden and a vertical fracture was found extending into the roof on mineback. Some minor horizontal fracture development was mapped, at the coal-rock interface, during the mining of this fracture. The pressure increased in the last 30 minutes of the treatment at a rapid rate, producing a log-log slope of 0.7 to 0.8 cycles per cycle. A gel-out at the fracture tip is believed responsible for this steep slope as a thick rubber-like gel was found in the last couple of metres of the vertical fracture mapped. A usable densitometer was not present during this treatment and the slurry concentrations have been found by adjusting the auger data to match the grab samples taken from the blender throughout the treatment.

The treatments in DDH 189 and 190 were similar in many respects. The high log-log slope recorded near the end of the treatment in DDH 189 is thought to be an expression of a gel-out or sand-out at the leading edge of the fracture in the coal. Fracture extension into the roof rock is believed to have been considerable in both treatments. The trace of the fractures in the roof contained offsets about every metre or so along the length of the traces. Pressure drops and proppant bridging at these offsets may provide a second explanation for the high rate of pressure increase measured, despite the fractures growing in height.

Mineback Results

The fracture created in ECC 87 was mined in November 1990 while the fractures in DDH 189 and 190 were mined in February through April 1992. ECC 87 was sited in front of a longwall and as the face advanced through the fracture, some data on fracture geometry could be collected for every cut (nominally a 900 mm slice) made. DDH 189 and 190 were located ahead of the development heading for the 202 panel maingate. These boreholes were located in-seam approximately in the center of 9 and 13 cutthroughs respectively. Close examination and mapping of these two fractures was restricted to the fracture left in the roof and in the coal ribs after the headings and cutthroughs were mined.

Data and Results

Figures 8, 9, and 10 show plan views of the fracture geometry mapped at each borehole. The outline of the headings is shown for the fractures located in the path of development mining.

The hydraulic fractures propagated along the primary cleat direction in the coal. The fractures in the roof rock, which were present at all three sites, followed the same general direction as the vertical fractures in the coal, but at most vertical sections were offset to one side or the other of the coal fractures. Setting an inflatable packer just above the coal seam may have induced stresses in the rock that promoted the growth of the hydraulic fracture in the roof. However, stress conditions measured at DDH 189 and 190 were such that growth of a vertical fracture into the roof rock was not unexpected. It should be noted that the full-scale hydraulic fracture treatment performed in ECC 90, which was located about 400 metres north of ECC 87, did not cause any fracture growth into the roof. Fracture propped extent in the coal as mapped is listed in Table 8 below. The values given for DDH 189 and 190 are estimates because the fracture in the coal died out between its trace on the south rib of the cutthrough and the east side of the belt roadway. The propped length to the SW was therefore taken as the distance from the borehole to a point halfway through the pillar in the strike direction of the fracture. Likewise, the propped fractures were present on the east rib of the traveling road at both borehole sites and 5 metres of propped length was added to the NE propped extent direction to account for unmined fracture length.

Representative vertical sections of the fracture mapped are shown in Figures 11, and 12. The mapping of ECC 87 generated a total of 33 vertical sections while mapping of the fractures in DDH 189 and 190 generated 5 vertical sections for each borehole.

The propped width and height data have been used to calculate the average propped width of each fracture at each mapped section. An overall average propped width was then found by weighting these vertical section averages by fracture length sections equal to the half the distance to the next vertical section to the NE and SW of the section mapped. Using an in-place unit weight for sand of 1.6 kg per litre, a weight of proppant in the coal and the percentage of the total proppant injected was found. Results of this calculation are given in Table 9 below.

In both DDH 189 and ECC 87, about 5 percent of the sand was left in the borehole. Similar amounts were likely left in the borehole in DDH 190, but because of post-fracturing flushing, well testing, and cementing operations, no fracturing sand was found in the borehole during the minethrough. In any event, it is likely that between 65 and 85 percent of the proppant was placed into fractures in the roof rock in these treatments.

APPLICATION OF EXPERIMENT RESULTS TO FULL SCALE TREATMENT DESIGN

Pressure responses recorded during the treatments, if interpreted according to classical methods, would imply that the hydraulic fractures created were contained in height during most of each treatment. This interpretation would lead to prediction of long fracture lengths with most of the sand injected ending up in a fracture in the coal seam. In reality, most of the fracture growth and sand occurred outside the coal seam in the roof rock.

One consistent feature of all three of these fractures and also of the full-scale fracture

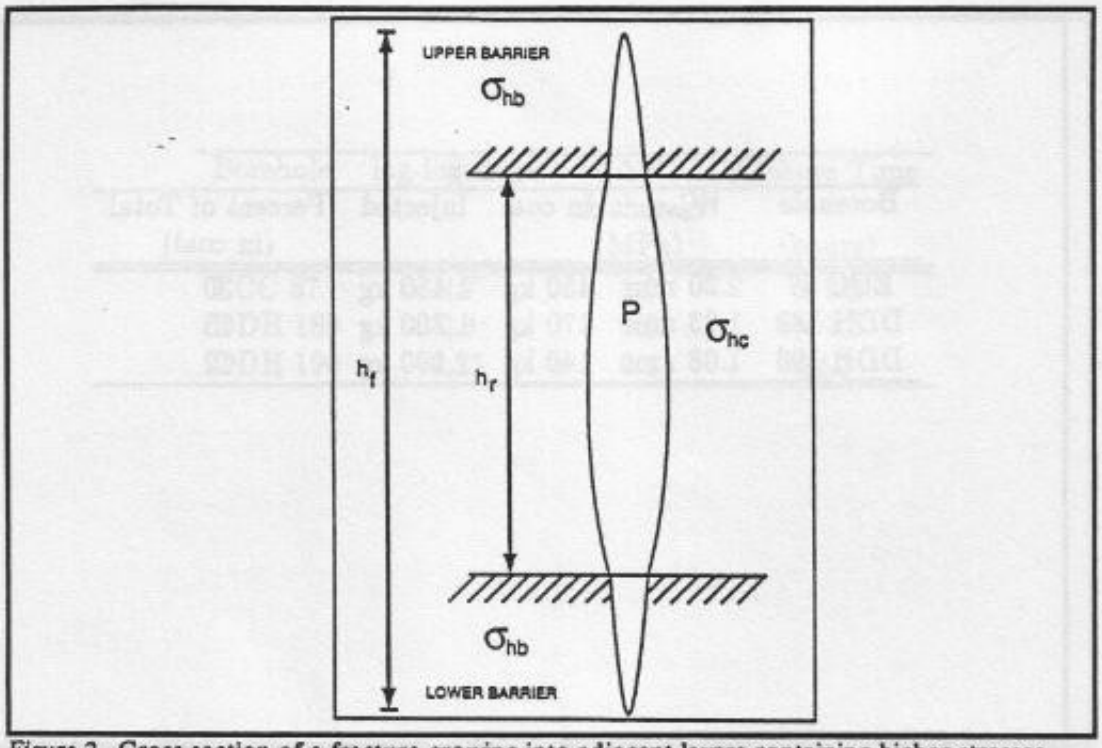

Figure 2. Cross section of a fracture growing into adjacent layers containing higher stresses

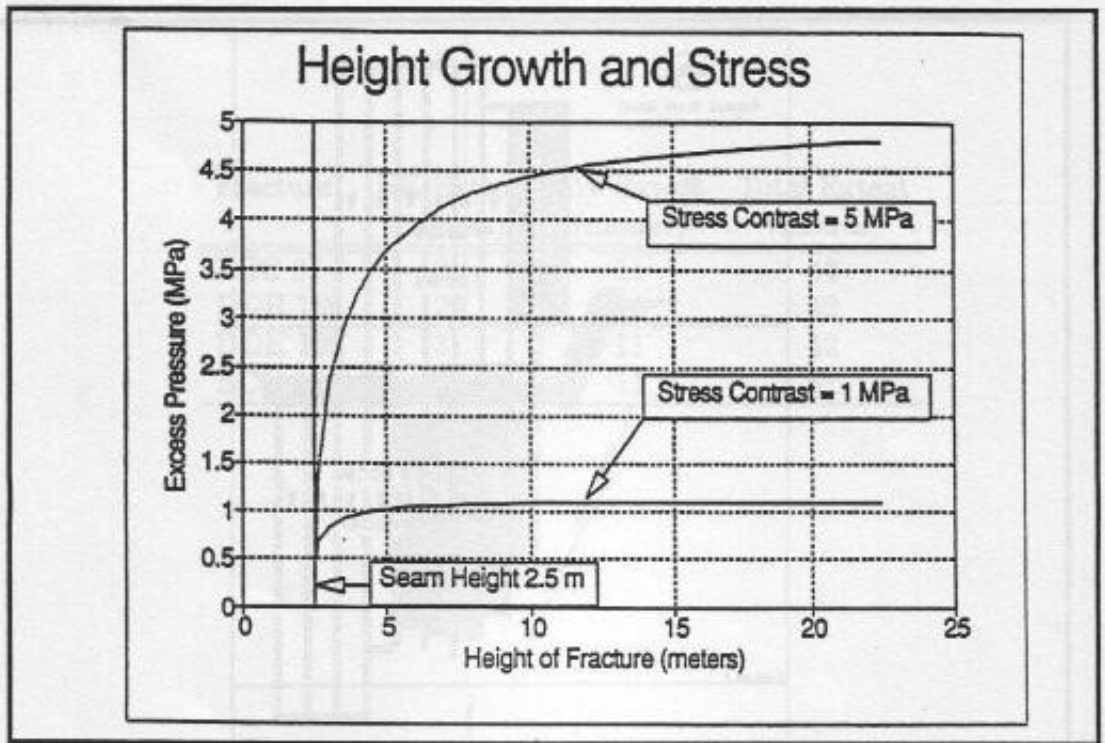

Figure 3. Height growth as a function of pressure for 1 and 5 MPa of stress contrast. The excess pressure is the closure stress in the coal seam minus the pressure in the fracture.

treatment done in ECC 90, is the asymmetry of the fractures formed. The propped extent of the fractures in the coal was consistently more to the NE than to the SW. Such uneven growth must reflect a property of the seam or rock layers that affected fracture propagation, sand transport, or fluid flow and pressure distribution inside the hydraulic fracture:

1. A tip screenout in one limb of the fracture could lead to asymmetric growth by blocking further extension in one direction. However, it seems unlikely that such a screenout would always occur in the SW branch. On the other hand, the consistent bias in fracture length to the NE, in the four treatments mined through in the German Creek seam, may not reflect a directional bias. It may be that some small event, such as proppant bridging or the crossing and formation of a single offset fracture may lead to less growth in one direction than the other and the fact that this growth limiting event occurred in the SW limb first in four out of four cases is explained by chance.

2. Fracture toughness of the coal would promote any asymmetry that developed if the fracture toughness were large enough to be the main factor controlling propagation (Jeffrey et al., 1987) and if its effect decreased with fracture half-length. This effect would be most pronounced in a plane-strain or KGD-type (Geertsam, 1989) or radial fracture geometries. In such geometries, the pressure needed to propagate the fracture deceases with the length or radius of the fracture. For example, in the KGD geometry, if the propagation is toughness dominated, the pressure decreases with the square root of fracture half length, L.

$$P_f = \frac{K_{Ic}}{\sqrt{\pi L}} \qquad (2)$$

Thus, if one limb of the fracture became slightly longer than the other, the tendency would be for this difference to increase further. This mechanism does not explain why the asymmetry was always biased toward the NE.

3. A second asymmetry-generating mechanism would involve the existence of a direction dependent flow resistance or propagation resistance. The fabric of the seam might be such that fracture toughness is less for propagation to the NE than to the SW or the flow channel might be such that frictional resistance is higher for flow in the SW direction than in the NE direction.

4. The longer limb of the fractures were consistently in the down-dip direction and a small additional pressure would arise in the long limb because of this elevation difference. In DDH 189 the up-dip fracture tip was 6 metres higher than the NE, down-dip tip. Such an elevation difference would lead to a pressure difference of only 0.02 MPa because part of the pressure difference arising from the greater slurry density (which was always less than 1.35) is compensated for by a similar gradient in reservoir pressure. Net pressures of 3 to 7 MPa were recorded in these treatments and superimposing a gravity-induced pressure component of 0.02 MPa in the NE limb does not provide an explanation for the preferred growth in that direction. In addition, the hydraulic fracture formed in U.S. Steel's well DHM-7 was mapped and found to be asymmetric, but it grew mostly in the up-dip direction (Boyer *et al.*, 1986).

Frictional forces are much larger than gravitational forces and dominate the extension process. Any accelerated growth down-dip associated with the gravitational pressure component requires higher flow rates in that wing. If the frictional pressure drop is taken, conservatively, as 2.0 MPa over 42 metres of fracture length, an estimate for the friction-induced pressure gradient is 0.048 MPa per metre. The gravity-induced pressure gradient is less than 0.0005 MPa per metre. For small changes in flow velocity, q, the flow velocity and pressure gradient are directly proportional (Geertsma, 1989).

$$\frac{dP}{dL} = \frac{64\mu}{\pi w^3 h} q \qquad (3)$$

Therefore, a one percent increase in flow rate will result in dissipating the gravity-induced pressure gradient in friction. Thus, at best, a 42 metre-long fracture (two symmetric 21 m wings) might grow asymmetrically because of gravity effects to be 21.25 metres long in the down-dip direction and 20.75 metres long in the SW direction.

Asymmetry in fracture propagation requires additional study because it may well be a common and important feature of fracture propagation in coal. The treating pressure to form an asymmetric fracture is expected to be slightly higher than a symmetric one. If the asymmetry develops during the slurry stages, then the wing taking most of the fluid will be prone to consuming all its pad fluid before the end of the treatment. In the worst case, one wing has the same pad volume but twice the slurry volume compared with a symmetric growth case.

Production Forecasts

A number of reservoir simulations were run to examine the effect of various sizes of hydraulic fracture treatments on degasification well production performance. The simulations were run on the COMETPC coalbed methane simulator (Sawyer *et al.*, 1990) and were intended to show the performance differences that might be expected between the fractures created in these experiments and ones that might be created by a full-scale treatment.

The comparison showed that the full-scale treatments resulted in gas and water production rates of 3 to 4 times those from the small treatments. However, only a relative small fraction of the gas in place was produced and, after three years, the full-scale treatments were predicted to have dropped to a gas rate of less than 5 mcfd.

The significance of these results depends on how representative the model and data is of reality. Additional basic data gathering and verification work would establish the simulation parameters more precisely. It would be especially valuable to have better desorption isotherm and relative permeability data. However, pilot well stimulation and production trials provide the ultimate test of the model.

Stress and Fracture Geometry

The in-situ state of stress affects hydraulic fracture growth in several ways. Hydraulic fractures propagate so that they open against the minimum principal stress. In cases where the minimum principal stress is vertical, the hydraulic fracturing operations result in the formation of a horizontal fracture and vertical fractures propagate when s_{min} is horizontal. When the principal stresses differ in magnitude by amounts larger than the excess pressure required to propagate a hydraulic fracture, the fracture propagation is planar. However, in situations where these differences in magnitude are less than the excess pressure needed to propagate the fracture further in the primary direction, a second or third fracture plane may form. Horizontal fractures overlying vertical fractures and vertical fractures in both the primary and secondary cleat directions are examples of multiplane fracture geometries that have been documented by mapping of hydraulic fractures formed in coal seams (Diamond, 1987; Jeffrey *et al.*, 1992).

Stress contrasts can act to either limit or promote fracture height growth. Height growth into low permeability rock above or below the target coal seam is undesirable because the propped fracture width and extent in the seam is reduced accordingly which reduces the effectiveness of the stimulation. In contrast, if one purpose of the stimulation is to fracture stimulate a number of vertically adjacent seams, height growth is desirable and strong stress barriers would make such a fracture design impractical. Horizontal stresses higher in magnitude than the vertical stress are common in eastern Australian coal basins. Fractures that are initiated or grow into such rock layers can be expected to reorient and become horizontal. Unless the rock is fairly permeable, such a fracture will be shielded from the coal seam, resulting in a poor stimulation. A horizontal fracture in or at the top of the coal may not effectively drain the entire seam because of low-permeability horizontal stone or clay layers in the seam. However, such relatively thin layers may not present effective barriers to fluid flow over large areas and it can be argued that horizontal fractures are effective in stimulating the seam because they connect across the more-permeable face cleat system.

The fracture geometry in the coal was affected by small features in the seam such as shear zones, bedding planes, clay layers, and stoney layers. Offsetting of the fracture to the left or right was common across the mid-seam shear zone. The fracture tended to be inclined or even horizontal in this zone. Stresses in shear zones and clay layers are

likely to be nearer lithostatic than in adjacent more competent coal and these stress differences may be responsible for reorientation, offsetting, or blunting the fracture. None of the fractures grew downward into the floor rock which is consistent with the higher magnitude stresses measured in those layers.

CONCLUSIONS

- Low injection rate experimental fractures are possible to carry out in coal seams. Evidence exists in two of the three treatment records for tip screenout or gel out behavior during later stages of the treatments.
- Higher treating pressures in ECC 87 correlate with the higher stresses in roof rock there and with propagation of fractures along both face and butt cleat directions.
- The fractures in the coal extended in the direction of s_{Hmax} as measured in the roof rock immediately above the seam.
- Height growth resulted from lower stresses in roof rock than in coal seam. Fracture extent in coal was reduced by height growth but fracture still extended vertically over the full seam height. Height growth may have been made more likely by the stresses induced in the roof rock by the inflatable packer set just above the top of the seam. No fracture growth into the floor rock was found, consistent with the higher magnitude stresses in the floor rock, and definite blunting of downward growth by a thin clay layer was mapped at 13 cut-through.
- Low temperature breakers must be used, as recommended by service companies, at these seam temperatures if the treatments are intended to stimulate water and gas production.
- The fractures did not adversely affect the mining.

ACKNOWLEDGMENTS

The project reported on here was funded directly by North Queensland Energy Pty. Ltd. and was supported through site access, drilling, logging, and general logistics by Capricorn Coal Management Pty. Ltd. Dowell Schlumberger provided fracturing materials at cost and gave engineering assistance. CSIRO Division of Geomechanics funded all other expenses for the project. The surface and mineback-mapping work were done by Mr Tim Ferguson, Mr Jeff Bride, Mr Steve Tsaganas, and Mr Owen Morros. The figures of the fracture as mapped were prepared by Mr Marco Cassetta. The contribution of all these organizations and people is gratefully acknowledged.

REFERENCES

Boyer II, C.M., P.B. Stubbs, F.C. Schwerer, R.G. Jeffrey, C.F. Brandenburg, and C.W. Byrer, (1986). Measurement of Coalbed Properties for Hydraulic Fracture Design and Methane Production, paper SPE 15258 presented at the 1986 Unconventional Gas Tech. Symp., Louisville, Kentucky.

Diamond, W.P., (1987). Characterization of Fracture Geometry and Roof Penetrations Associated with Stimulation Treatments in Coalbeds, paper 8752 in the proceedings of the 1987 Coalbed Methane Symposium, Tuscaloosa, Alabama.

Enever, J.R., and B. Wooltorton, (1986). Stress Measurement at Gregory and German Creek Mines, Central Bowen Basin, Queensland, Site Investigation Report No. 23, CSIRO Div. of Geomechanics.

Geertsma, J., (1989). Two-Dimensional Fracture-Propagation Models, chapter 4 in *Recent Advances in Hydraulic Fracturing*, SPE monograph vol. 12, J.L Gidley editor-in-chief.

Heller, R.A. and G.W. Swift, (1971). Solutions for the Multilayer Timoshenko Beam, Report VPI-E-71-12, Department of Engineering Mechanics, College of Engineering, Virginia Polytechnic Institute and State University.

Jeffrey, R.G., L. Vandamme, and J.-C. Roegiers, (1987). Mechanical Interactions in Branched or Subparallel Hydraulic Fractures, SPE 16422 presented at the 1987 SPE/DOE Symposium on Low Permeability Reservoirs, Denver, Colorado.

Jeffrey, R.G., R.P. Byrnes, P.A. Lynch, and D.J. Ling, (1992). An Analysis of Hydraulic Fracture and Mineback Data for a Treatment in the German Creek Coal Seam, paper SPE 24362 presented at the SPE Rocky Mt. Regional Meeting, Casper, Wyoming.

Nolte, K.G., and M.B. Smith, (1981). Interpretation of Fracturing Pressures, **JPT**, Sept. 1981.

Nolte, K.G., (1989). Fracture-Pressure Analysis, chapter 14 in *Recent Advances in Hydraulic Fracturing* SPE monograph vol. 12,J.L Gidley editor-in-chief.

Puri, R., G.E. King, and I.D. Palmer, (1991). Damage to Coal Permeability During Hydraulic Fracturing, paper 9169 in proceedings of the 1991 Coalbed Methane Symposium, Tuscaloosa, Alabama.

Sawyer, W.K, G.W. Paul, and R.A. Schraufnagel, (1990). Development and Application of a 3D Coalbed Simulator, paper No. CIM/SPE 90-119 presented at the International Technical Meeting of CIM and SPE, Calgary, Alberta.

Simonson, E.R., A.S. Abou-Sayed, and R.J. Clifton, (1978). Containment of Massive Hydraulic Fractures, SPEJ, Feb. 1978.

Warpinski, N.R.,(1991). Hydraulic Fracturing in Tight, Fissured Media, JPT, Feb. 1991.

Material	E (MPa)	ν	Compressive Strength (MPa)
ECC 87			
Roof rock	24,000	0.22	56
Coal	2,000	0.35	–
Floor rock	24,400	0.15	50
DDH 189			
Roof rock	31,000	0.29	73
Coal	2,000	0.35	–
Floor rock	22,800	0.10	82
DDH 190			
Roof rock	25,200	0.13	40
Coal	2,000	0.35	–
Floor rock	20,600	0.14	79

Table 1. Mechanical properties

Well	Reservoir Pressure (MPa)	Permeability (md)	Depth of Seam (metres)
ECC 87	0.2	1 to 5	216.7
DDH 189	0.75	1.1	198.4
DDH 190	1.08	4.2	193.5
DDH 163†	0.75	1 to 5	214.7

† – No fracture experiment, well test only in this borehole.

Table 2. Well test results

Test Interval	σ_{Hmax} (MPa)	σ_{Hmin} (MPa)	Orientation of σ_{Hmax}	Description
ECC 87				
206.8–207.4 m	10.3	5.5	N24E	Sandstone. Vertical fracture.
210.25–210.85 m	10.3	5.0	N49E	Sandstone.
215.2–217.5 m	–	2.5	N41E	German Creek coal seam. σ_V = 5.1 MPa.
219.7–220.3 m	> 5.1	> 5.1	–	Horizontal fracture.
DDH 189				
187.8–188.5 m	12–14	4.5	N26E	Sandstone. Vertical fracture.
192.4–193.1 m	4	2.4	N41E	Laminated sandstone and siltstone. En echelon vertical fracture.
197.4–199.5 m	–	3.1	N40E	German Creek coal seam. σ_V = 4.6 MPa.
202.0–202.7 m	–	> 6	N56E	Laminated sandstone and siltstone. Vertical fracture turning horizontal.
DDH 190				
185.6–186.2 m	–	1.9	N17E	Large vertical fracture.
187.2–187.9 m	–	1.7	–	
192.6–194.5 m	–	2.0–3.0	N34E	German Creek coal seam. σ_V = 4.5 MPa.
196.5–197.2 m	–	> 6	–	Horizontal fracture.

Table 3. Summary of stress measurement results

Borehole	Geometry	Leakoff Coeff. $\frac{m}{\sqrt{min}}$
ECC 87	KGD	0.0020†
DDH 189	KGD	0.0013
DDH 190	KGD	0.0010

† Linear gel.

Table 4. Leakoff coefficients from minifrac tests

Parameter	Small-Scale	Full-Scale	Ratio $\left(\frac{\text{Full}}{\text{Small}}\right)$
Volume	15,000 litres	400,000 litres	26.7
Injection Rate	150 lpm	4,800 lpm	32.0
Fluid type	crosslinked gel	crosslinked gel	–
Proppant type	sand	sand	–
Proppant size	40/70 mesh	12/20 mesh	4.0††
Cost	$20,000†	$150,000	7.5

† Treatment only.
†† Based on average grain size.

Table 5. Comparison of small- and full-scale treatments

Borehole	Inj. Rate (litres/min)	Volume Injected (litres)	Proppant Injected (kg)	Max. Press. (MPa)
ECC 87	100	12,200	1,480	10.3
DDH 189	93	14,100	1,300	7.0
DDH 190	149	13,600	1,190	5.5

Table 6. Experimental fracturing treatments

Borehole	log-log slope	ΔP at shut-in (MPa)	Closure Time (hours)
ECC 87	0.7	1.0	> 3.3
DDH 189	0.8	0.5	> 7.5
DDH 190	0.25	0.4	14.3

Table 7. Fracture treatment characteristics

Fracture	NE Extent (metres)	SW Extent (metres)	Total Extent (metres)
ECC 87	31	11	42
DDH 189	26	16	42
DDH 190	31	11	42
ECC 90	80	11	91

Table 8. Summary of propped fracture extent mapped in coal

Borehole	W_{ave}	In coal	Injected	Percent of Total (in coal)
ECC 87	2.20 mm	450 kg	1,480 kg	30
DDH 189	1.33 mm	170 kg	1,300 kg	13
DDH 190	1.08 mm	140 kg	1,190 kg	12

Table 9. Proppant placed in coal seam

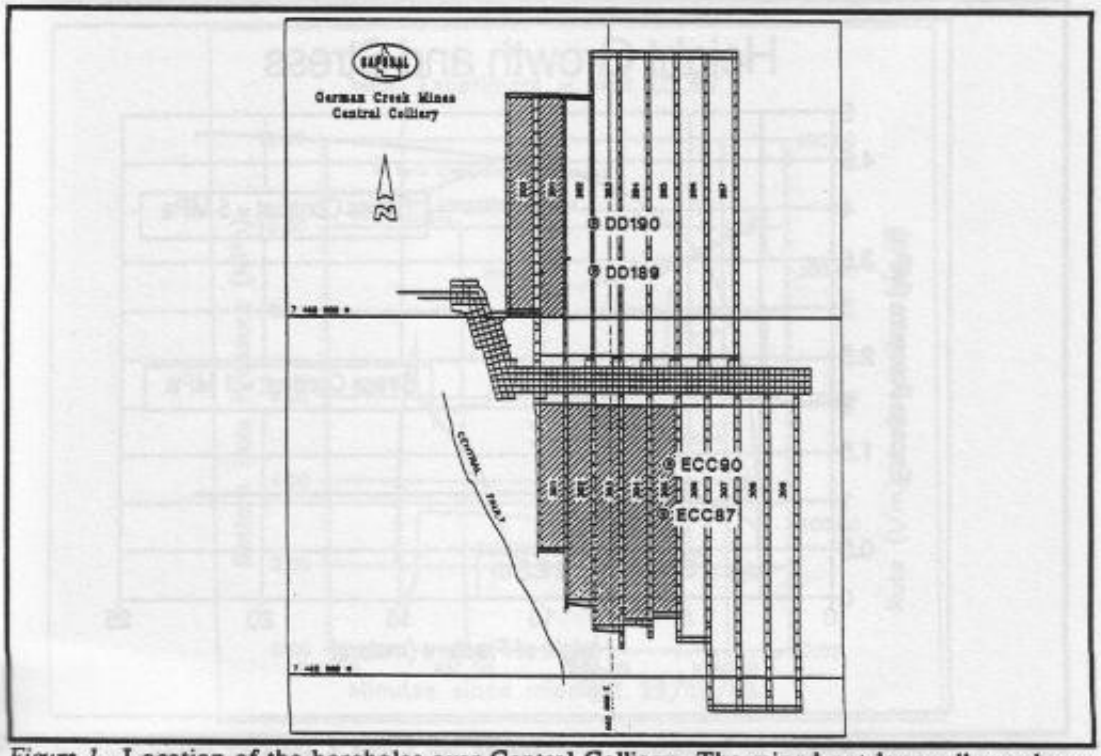

Figure 1. Location of the boreholes over Central Colliery. The mined-out longwall panels are shown as of 1 September 1992

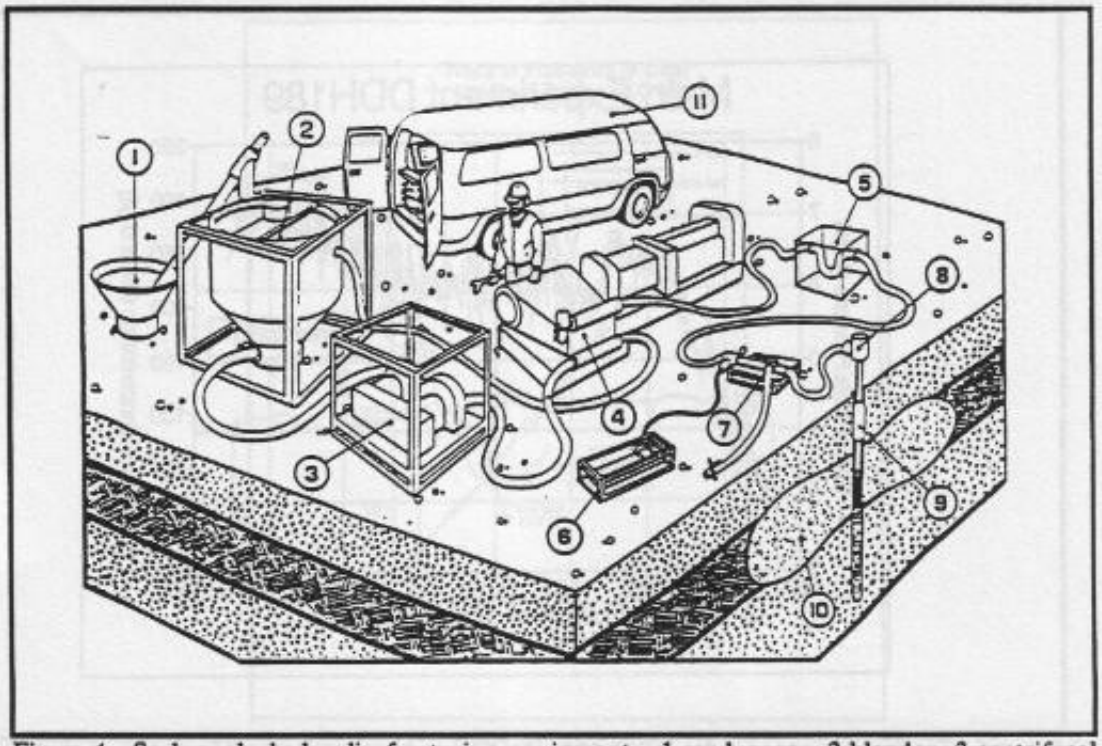

Figure 4. Scale-scale hydraulic fracturing equipment. 1-sand auger, 2-blender, 3-centrifugal pumps, 4-triplex pump, 5-flow and density meter, 6-activitor pump, 7-shut-in and flow back valves, 8-well head, 9-packer and pressure sensor, 10-hydraulic fracture, 11-instrumentation van

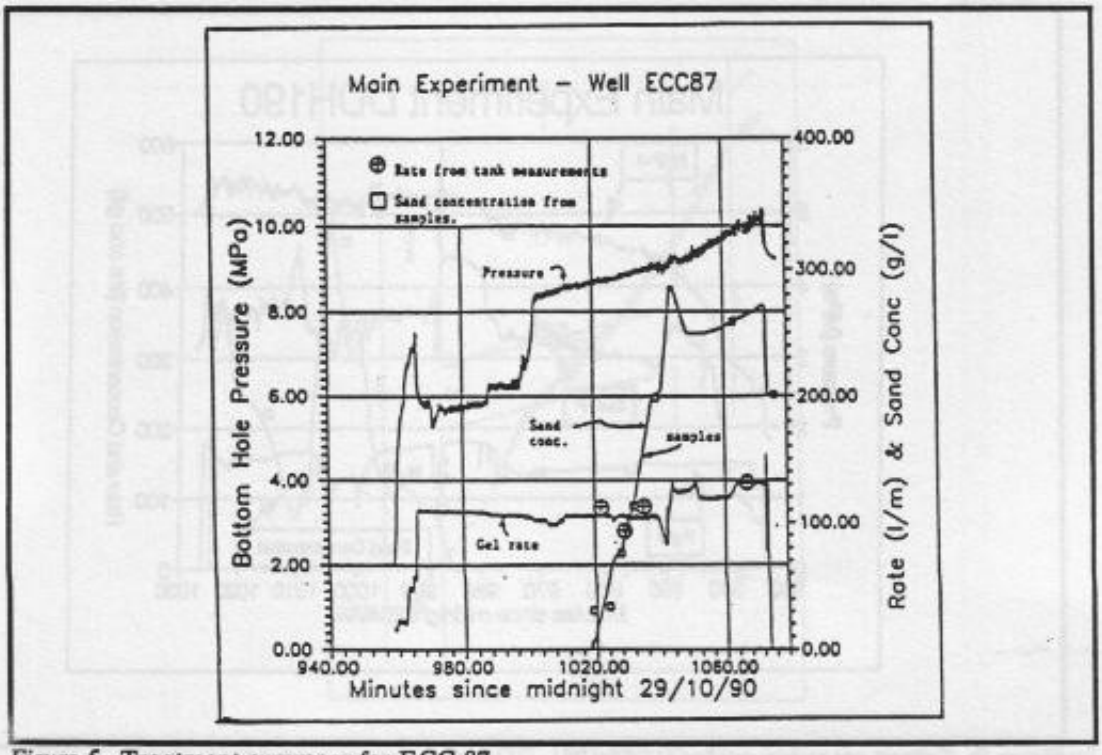

Figure 5. Treatment summary for ECC 87

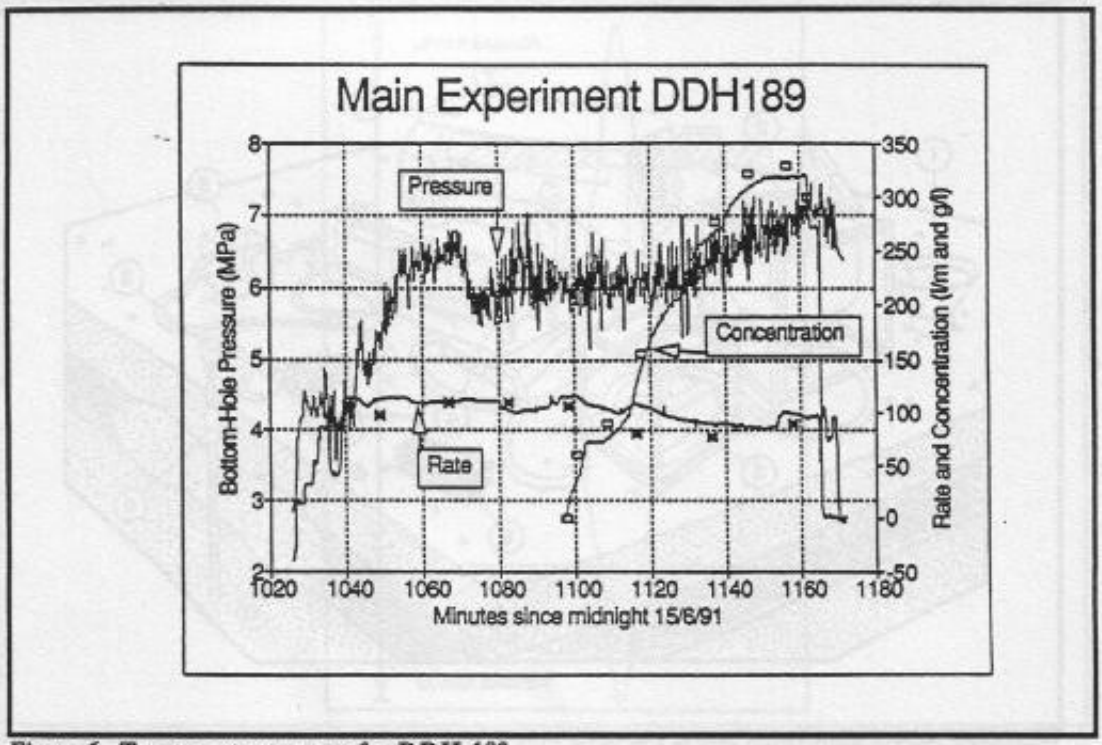

Figure 6. Treatment summary for DDH 189

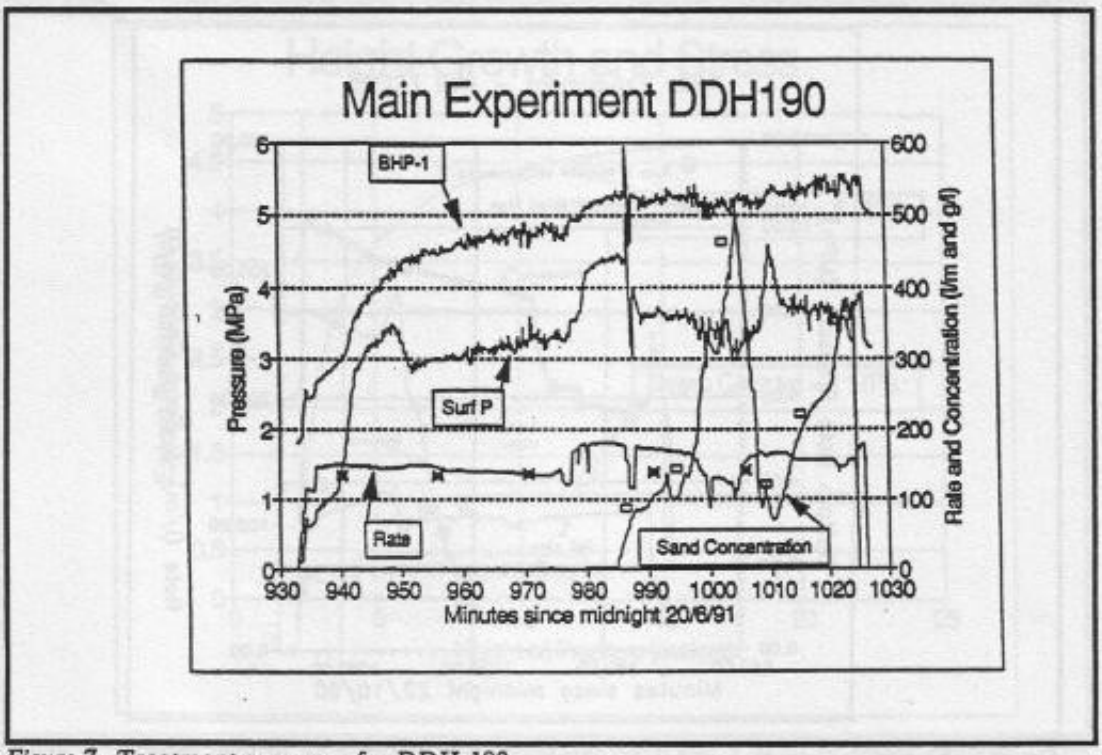

Figure 7. Treatment summary for DDH 190

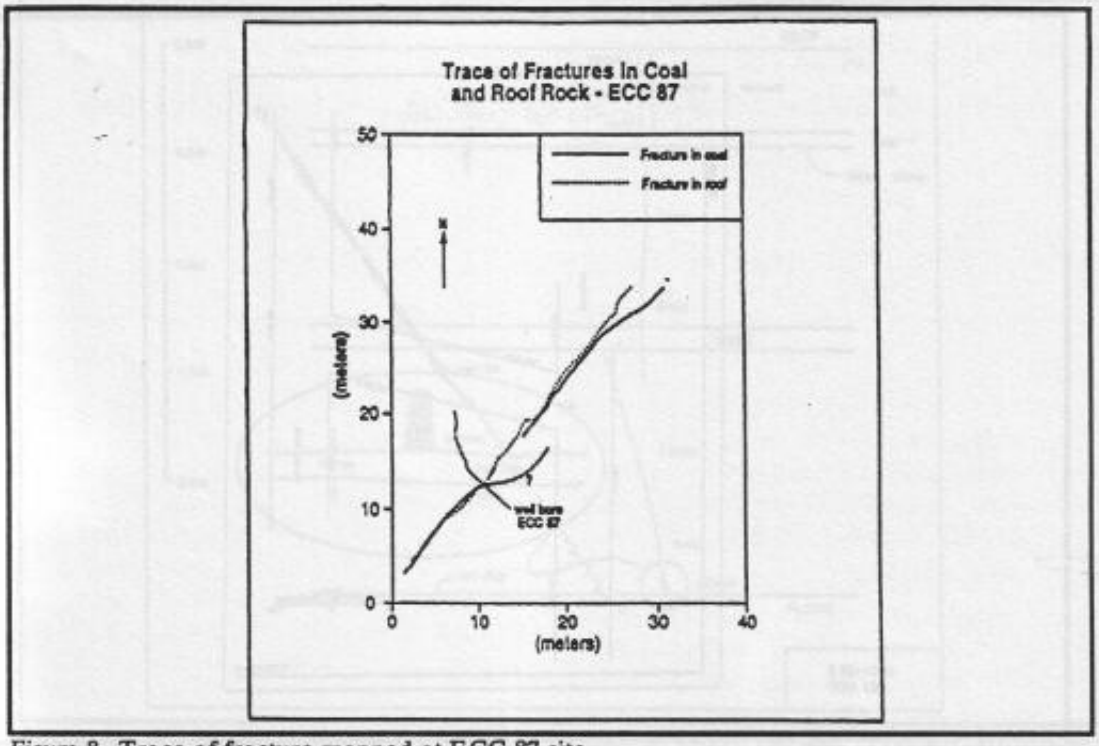

Figure 8. Trace of fracture mapped at ECC 87 site

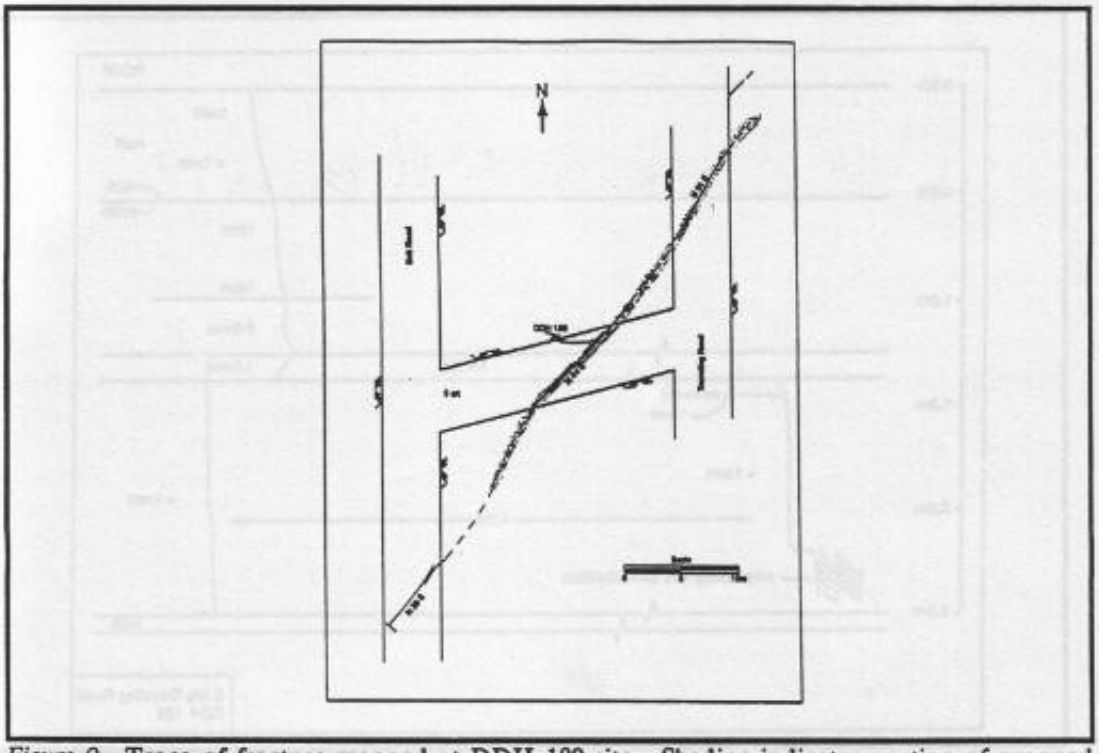

Figure 9. Trace of fracture mapped at DDH 189 site. Shading indicates portion of propped fracture trace mapped in coal

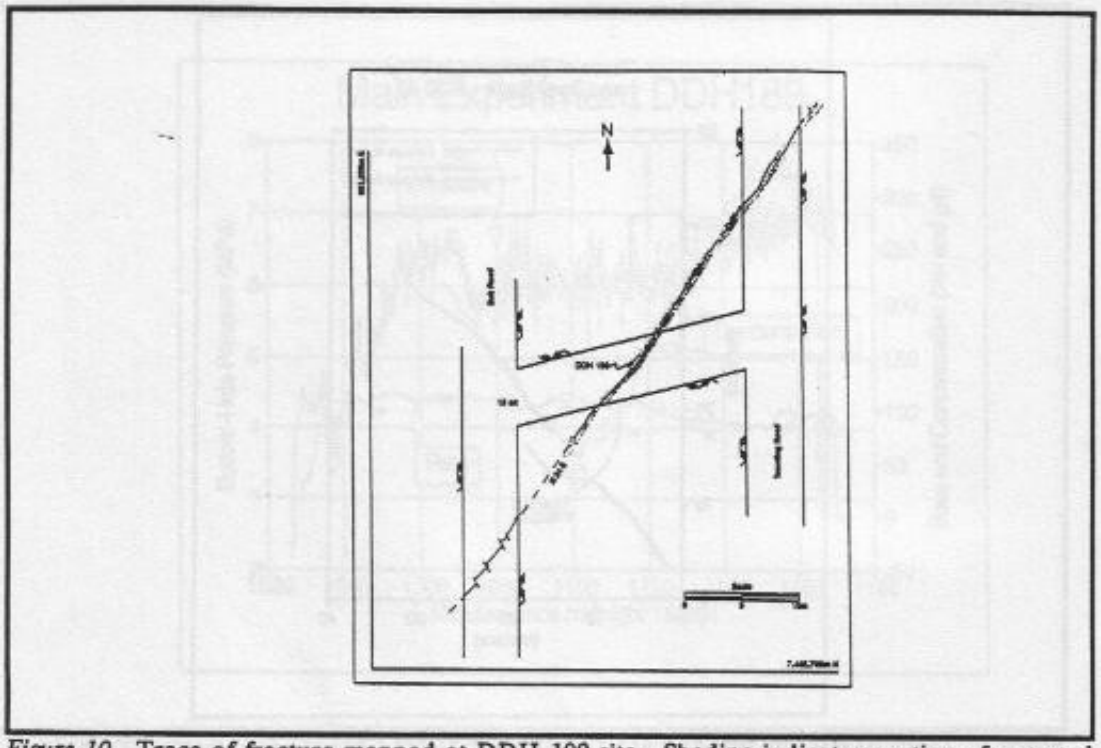

Figure 10. Trace of fracture mapped at DDH 190 site. Shading indicates portion of propped fracture trace mapped in coal

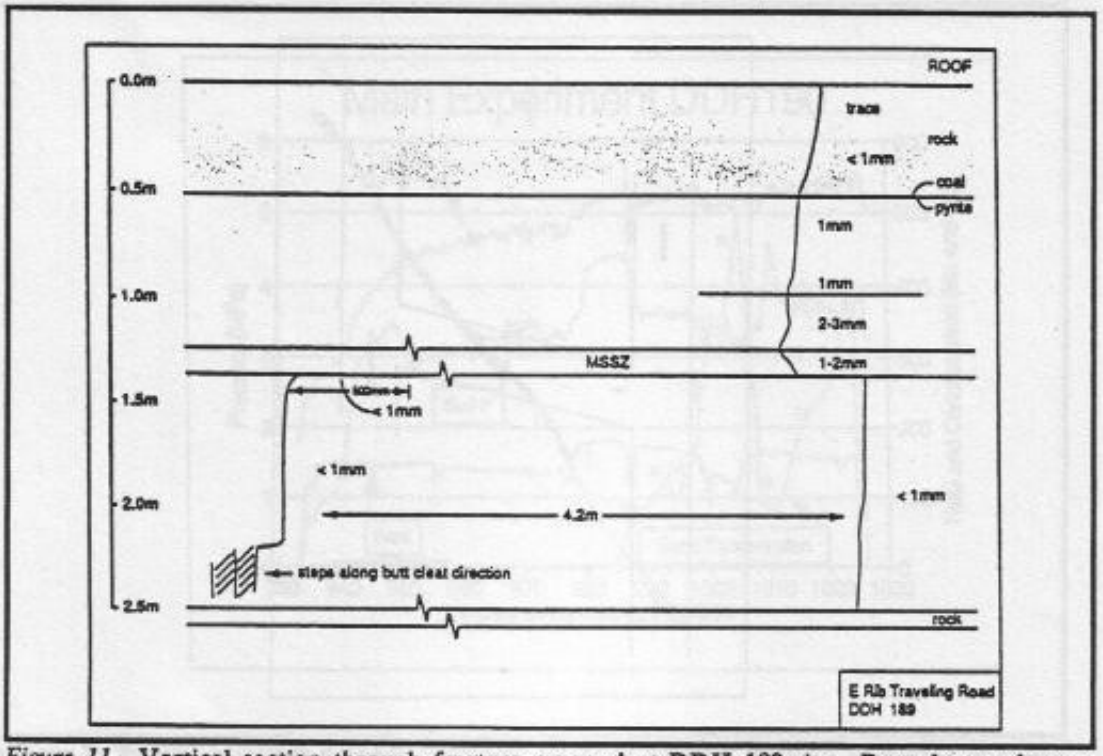

Figure 11. Vertical section through fracture mapped at DDH 189 site. Butt-cleat and some horizontal fracturing was found in fracture branch to the north of main fracture.

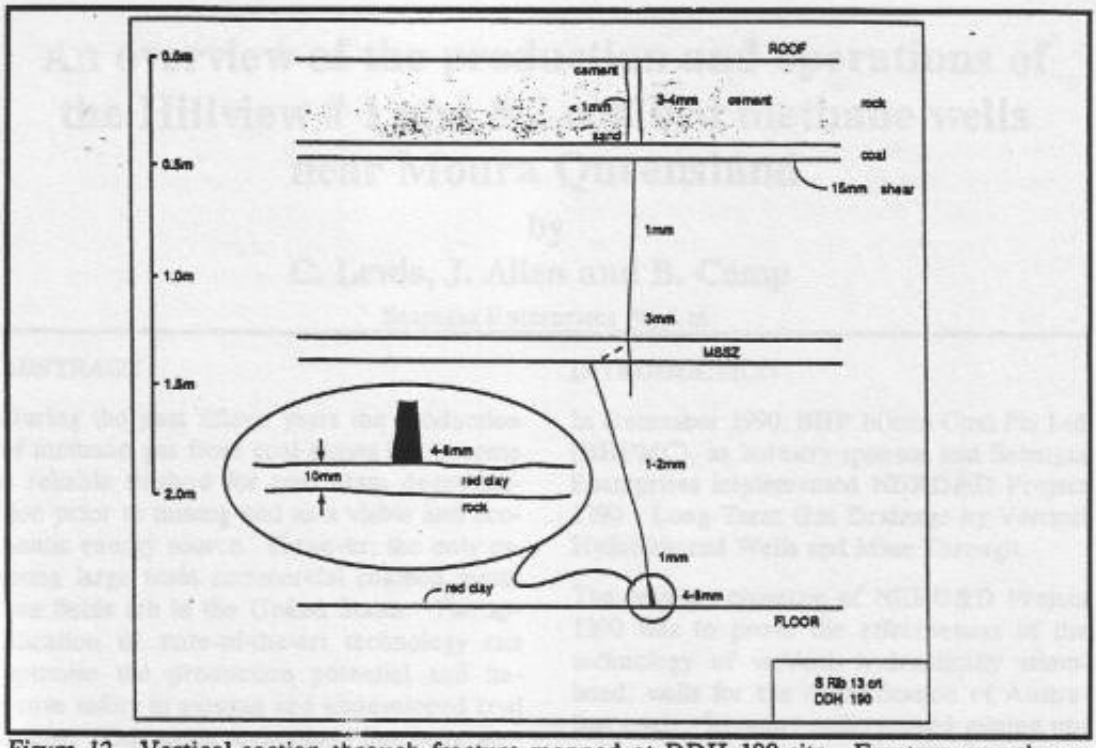

Figure 12. Vertical section through fracture mapped at DDH 190 site. Fracture growth was blunted by a 10 mm thick clay layer at the floor